We are IntechOpen, the world's leading publisher of Open Access books Built by scientists, for scientists

5,800
Open access books available

142,000
International authors and editors

180M
Downloads

Our authors are among the

154
Countries delivered to

TOP 1%
most cited scientists

12.2%
Contributors from top 500 universities

BOOK CITATION INDEX
CLARIVATE ANALYTICS
INDEXED

WEB OF SCIENCE™

Selection of our books indexed in the Book Citation Index
in Web of Science™ Core Collection (BKCI)

Interested in publishing with us?
Contact book.department@intechopen.com

Chapter

Biophysical and Biochemical Approaches for R-Loop Sensing Mechanism

Na Young Cheon, Subin Kim and Ja Yil Lee

Abstract

An R-loop is a triple-stranded nucleic acid structure consisting of a DNA–RNA hybrid and a displaced single-stranded DNA. R-loops are associated with diverse biological reactions, such as immune responses and gene regulation, and dysregulated R-loops can cause genomic instability and replication stress. Therefore, investigating the formation, regulation, and elimination of R-loops is important for understanding the molecular mechanisms underlying biological processes and diseases related to R-loops. Existing research has primarily focused on R-loop detection. In this chapter, we introduce a variety of biochemical and biophysical techniques for R-loop sensing and visualization both *in vivo* and *in vitro*, including single-molecule imaging. These methods can be used to investigate molecular mechanisms underlying R-loop search and identification.

Keywords: R-loop, genetic instability, R-loop sensing, and single-molecule imaging

1. Introduction

1.1 History of R-loops

R-loops are three-stranded nucleic acid structures consisting of a DNA–RNA hybrid and a displaced single-stranded (ss) DNA. They were first described in 1976 by Thomas *et al*., who observed a hybridized form of ribosomal RNA and ribosomal DNA of *Saccharomyces cerevisiae* 26S [1]. Structurally, RNA–DNA hybrids adopt an A-form structure [2, 3]. The structure of an R-loop formed with RNA polymerase or CRISPR-Cas9 shows that R-loops have a helical RNA–DNA hybrid structure and a dissociated ssDNA [4–7].

1.2 Biological functions of R-loops

RNA–DNA hybrids can be formed from GC-rich clusters during transcription or primer synthesis of DNA replication [2, 8]. Because nucleic acid strands are stabilized when they form a double-stranded conformation, the nascent RNA is hybridized to the template DNA strand when the double-stranded (ds)DNA is denatured during replication or transcription [2]. Therefore, R-loops can form at any time when there

is a chance that RNA can be annealed with its template DNA. The thread-back model proposes that R-loop formation stems from the annealing of RNA with DNA when the DNA left behind the transcriptome is negatively supercoiled and unwound [9]. Previous studies support this model [10–13]. Incomplete transcription elongation and termination also induce RNA–DNA hybrid formation, and the denaturation of duplex DNA by negative supercoiling increases R-loop formation.

R-loops have multiple roles in diverse biological reactions (**Figure 1**). First, R-loops induce genetic rearrangements in B-cells during immunoglobulin class switching [14]. R-loop formation is promoted by transcription through switched immunoglobulin loci, and the R-loop provides a ssDNA substrate for activation-induced deaminase (AID), which converts cytosine to uracil in both DNA strands. Uracil is subsequently removed by uracil glycosylase, and apurinic/apyrimidinic endonuclease makes nicks at the abasic sites and induces DNA double-strand breaks. During DNA double-strand break repair, the immunoglobulin locus is rearranged to change the level of antibodies generated. R-loops can also regulate both the activation and termination of transcription. Most human promoters are associated with CpG islands [15]. Ginno *et al*. demonstrated that R-loops are located at promoter sites that have CpG islands and proposed that R-loops protect the template DNA strand from gene-silencing methylation [16]. R-loop stabilization at the promoter region also regulates transcription. Flowering Locus C (FLC) is a transcription repressor of *Arabidopsis thaliana* that is regulated by COOLAIR through antisense transcription. Sun *et al*. found that the homeodomain protein AtNDX stabilizes R-loops by binding their displaced ssDNA at the *COOLAIR* promoter, thus inhibiting *COOLAIR* transcription and regulating *FLC* expression [17]. Antisense transcription-mediated R-loop formation at the *Vimentin* (*VIM*) promoter induces local chromatin decondensation and enhances gene expression [18]. R-loops also play a role in chromatin organization. For example, they are tightly linked to H3 S10 phosphorylation, which is a mark of chromatin condensation [19]. R-loops regulate both transcription
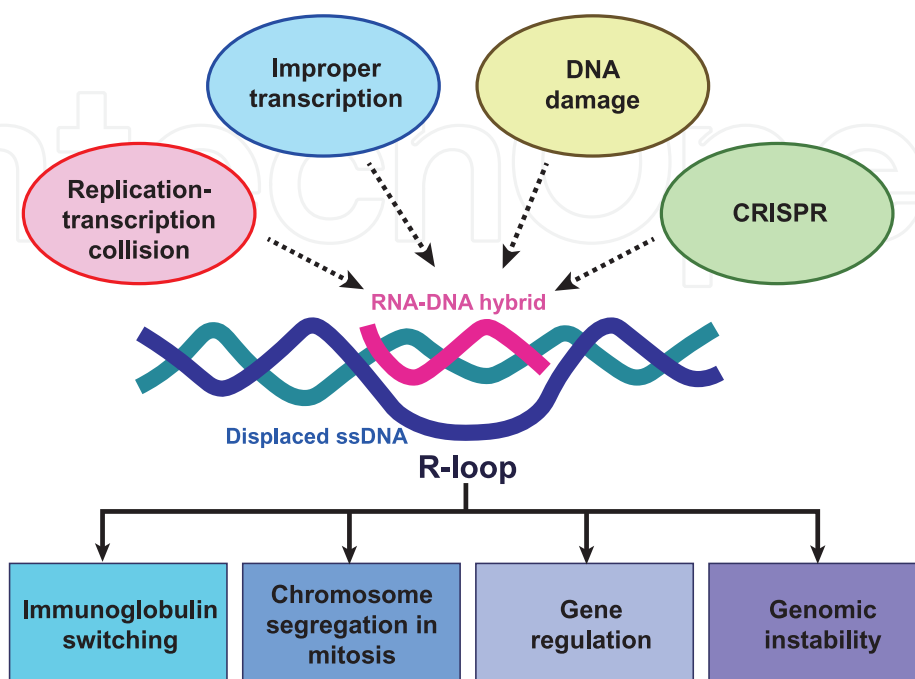
Figure 1.
The causes and consequences of R-loop formation.

initiation and termination [20]. Skourti-Stathaki *et al.* proposed a pause-dependent transcription termination mechanism mediated by R-loops and H3K9me2. R-loops are formed in transcription termination regions containing GC-rich sequences and facilitate antisense RNA transcription, inducing dsRNA for RNA interference factors, and they recruit G9a/GLP for the methylation of H3K9 along with HP1γ, which terminates transcription [21]. In addition to research by Skourti-Stathaki and colleagues, other studies suggest that R-loops can regulate transcription termination by RNA polymerase pausing [22, 23]. R-loops also occur at telomeres. Telomeric-repeat-containing RNAs (TERRAs) are noncoding RNAs transcribed from eukaryotic telomeres [24]. During telomerase-mediated telomere elongation in *rat1–1* mutant *Saccharomyces cerevisiae*, TERRAs form RNA–DNA hybrids and inhibit telomerase function [25]. In addition, the THO complex maintains yeast telomeres by suppressing R-loops generated by TERRAs [26].

1.3 R-loops, genomic instability, and human diseases

Despite the multiple roles of R-loops in normal cellular processes described above, they are also considered a form of DNA damage that can threaten genomic maintenance and integrity. In particular, the displaced ssDNA in an R-loop can increase genomic instability because it is a good endonuclease substrate [13, 27]. R-loops also induce replication stress. When the displaced ssDNA is broken, the replication fork stops at the R-loop. The RNA–DNA hybrid itself can block the progression of replication forks, and DNA polymerases may become trapped at R-loops [13, 28, 29]. Such replication stresses will activate DNA repair pathways, which might cause chromosome rearrangement [29].

Genomic instability that stems from R-loops may also contribute to some human diseases. Although there is no apparent evidence that R-loops are directly associated with disease, efforts to show causality between R-loops and disease have increased [30]. Some genetic disorders are caused by gene-specific repeats. R-loop formation is highly probable in tandem repeat sequences with high GC content and could change the repeat length. In particular, trinucleotide repeat expansion is a major cause of neurological and neuromuscular diseases, such as Huntington's disease and fragile X syndrome [31, 32]. It has been proposed that R-loops are associated with other neurological disorders, including amyotrophic lateral sclerosis, Aicardi-Goutières syndrome, and Prader-Willi syndrome [33–35]. R-loops also appear to be associated with cancer. *BRCA* genes, which are involved in DNA double-strand break repair via homologous recombination, are intimately associated with breast and ovarian cancer, and BRCA2 prevents R-loop accumulation [36, 37]. VIM is a member of the intermediate filament family and associated with different types of cancer. In colon cancer, the *VIM* promoter is hypermethylated and *VIM* expression is silenced. In normal cells, the gene is activated by R-loop formation in the promoter region, raising the possibility that transcription regulation by R-loops related to cancer development [18].

1.4 R-loop prevention and elimination

As described above, R-loops can cause genomic instability unless they are resolved, so they must be properly regulated. Several proteins are involved in R-loop prevention or elimination, such as RNase H, DNA TOP1, and Sen1 [38]. For example, RNase H directly removes R-loops by specifically degrading the RNA in RNA–DNA hybrid structures [39]. RNA helicases also resolve R-loops by unwinding RNA–DNA

hybrid structures [40]. Because negative supercoiling promotes R-loop formation, topoisomerases play a key role in preventing R-loops [41]. In the case of replication fork stalling due to R-loops, FANCD2 recruits RNA processing enzymes such as hnRNP U and DDX47 to resolve R-loops at the stalled fork [42].

2. *In vivo* R-loop assays

Visualizing R-loop formation is important for understanding R-loop metabolism. Because R-loops basically consist of nucleic acids, distinguishing R-loop from ds- and ss-DNA or RNA using existing DNA staining or visualization methods is challenging. S9.6 is an antibody specific to an RNA–DNA hybrid, which was developed in 1986 and rapidly advanced R-loop-related research [43]. This antibody is commonly used to detect R-loops both *in vivo* and *in vitro* [44–47].

Currently, the most popular R-loop characterization technique is DNA–RNA immunoprecipitation sequencing (DRIP-seq), in which RNA–DNA hybrid strands are immunoprecipitated with S9.6 and then sequenced (**Figure 2**, [47, 48]). DRIP-seq was first adopted for profiling CpG island promoters, where R-loops are predominantly formed [16]. This method revealed that genes containing terminal GC-rich sequences form R-loops at their 3′-end, suggesting that R-loops contribute to efficient transcription termination [20]. The DRIP-seq technique has been further improved; S1 nuclease treatment prior to DRIP-seq can stabilize the DNA–RNA hybrid because S1 removes the displaced ssDNA, thus improving the resolution [49]. In conventional DRIP-seq, it is assumed that the content of R-loops or RNA–DNA hybrids does not vary depending on cell type and growth condition. For appropriate comparison, quantitative differential DNA–RNA immunoprecipitation sequence (qDRIP-seq) uses synthetic RNA–DNA hybrids as internal standards and facilitates comparison between different conditions with high resolution and sensitivity [50]. Although DRIP-seq is a very robust and well-characterized technique, it can only measure the ensemble average level of R-loops. However, single-molecule R-loop footprinting (SMRF-seq) can reveal the R-loop population via chemical reactivity of ssDNA at the single-molecule level. Malig *et al*. developed SMRF-sequencing based on non-denaturing bisulfite conversion [51, 52]. Sodium bisulfite treatment converts unpaired cytosines to uracils on ssDNA. In R-loops, only one strand is unpaired and exposed to bisulfite, whereas the complementary strand is protected by RNA. Thus, the PCR product of the displaced single strand in an R-loop has a converted sequence of cytosines to thymines, which is a footprint of the R-loop. PCR products are rapidly sequenced using a single-molecule real-time sequencing technique [53]. This approach enables characterization of the individual footprints of R-loops on long-range genomes at high resolution, even at the single-molecule level.

Fluorescently labeled S9.6 can be used as an R-loop probe in microscope imaging at the cellular level (**Figure 3a**). The brief procedure is following. K562 cells were pelleted after trypsinization for detaching cells from the plate. Supernatant was discarded to approximately 300 ul, and cell pellets were resuspended. 5 ml of 37°C pre-warmed 75 mM KCl solution was added in a drop-wise manner while the resuspended cells were slowly agitated. After the cells were incubated at 37°C for 14 min, five or six drops of fresh ice-cold fixative solution (3,1 methanol:acetic acid) were added to the cells, which were centrifuged again. Supernatant was discarded to approximately 300 ul, and cell pellets were resuspended. The cells were treated on ice with 5 ml of ice-cold fixative solution in a drop-wise manner. After washed once with
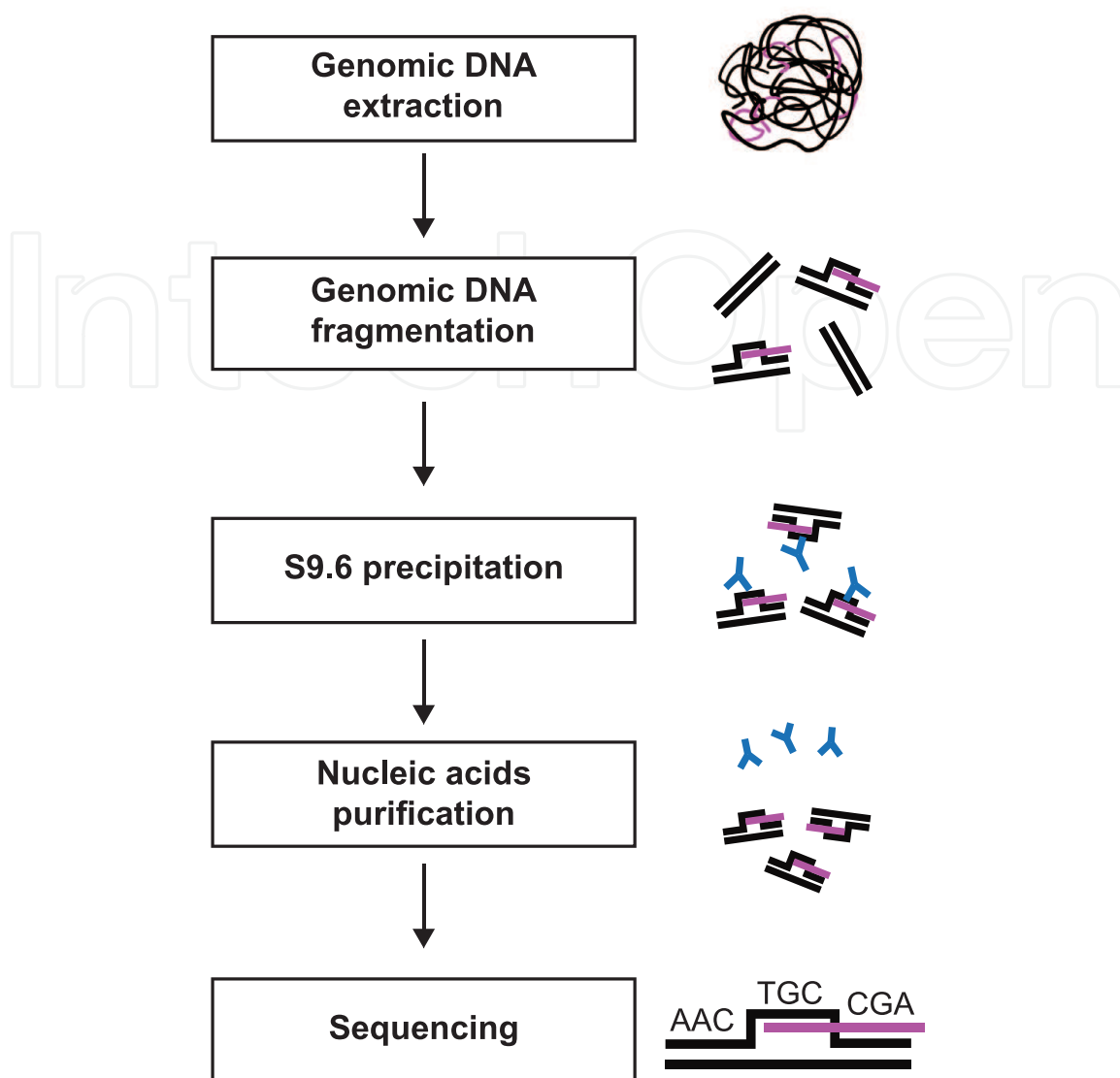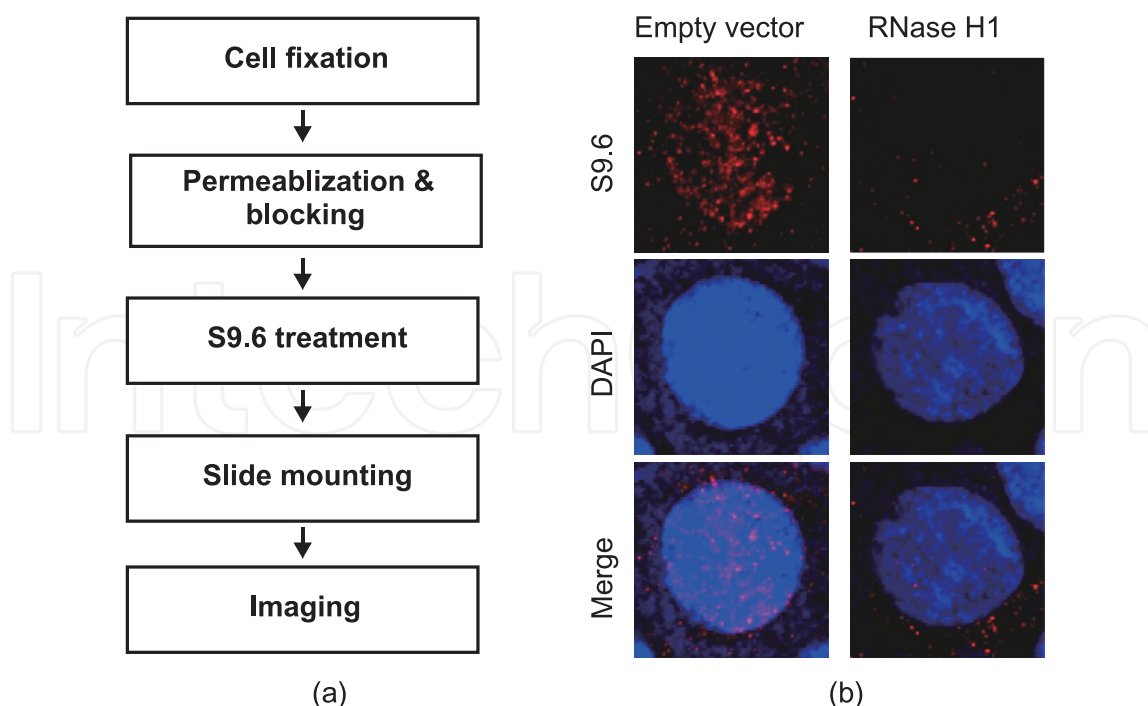
Figure 2.
The flow chart of DRIP-seq. Step 1: whole-genomic DNA containing R-loops is extracted from cells.
Step 2: extracted genomic DNA is fragmented by various types of restriction enzymes. Step 3: R-loops containing
RNA–DNA hybrids are precipitated with S9.6 antibodies. Step 4: S9.6 antibodies are eliminated by proteinase K
treatment, and R-loops are purified by phenol-chloroform extraction followed by ethanol precipitation. Step 5:
precipitated R-loops are sequenced.

fixative solution, the cells were spread onto a clean slide followed by 1 min incubation in 95°C steam for drying. The slide was immediately treated with blocking buffer (1x PBS, 5% BSA, 0.5% Triton X-100) and incubated at room temperature for 1 hr. The slide was successively treated with S9.6 antibody (1500) in blocking buffer at 4°C overnight. After residual S9.6 antibody was washed three times with washing buffer (1x PBS supplemented with 0.1% Triton X-100), the slide was treated with mouse AlexaFluor 594-conjugated secondary antibody at room temperature for 1 hr. The unbound secondary antibody was washed three times with washing buffer, and then the cells were stained with 4,6 diamidino-2-phenylindole (DAPI) and mounted using Vectashield (Vector Laboratories). Finally, the cells were imaged using a fluorescence microscope.

The use of immunofluorescence with S9.6 can allow visualization of the intracellular locations of RNA–DNA hybrids, even in mitochondria [54–56]. Furthermore, R-loop detection by S9.6 is ensured by RNase H1 overexpression (**Figure 3b**). R-loops
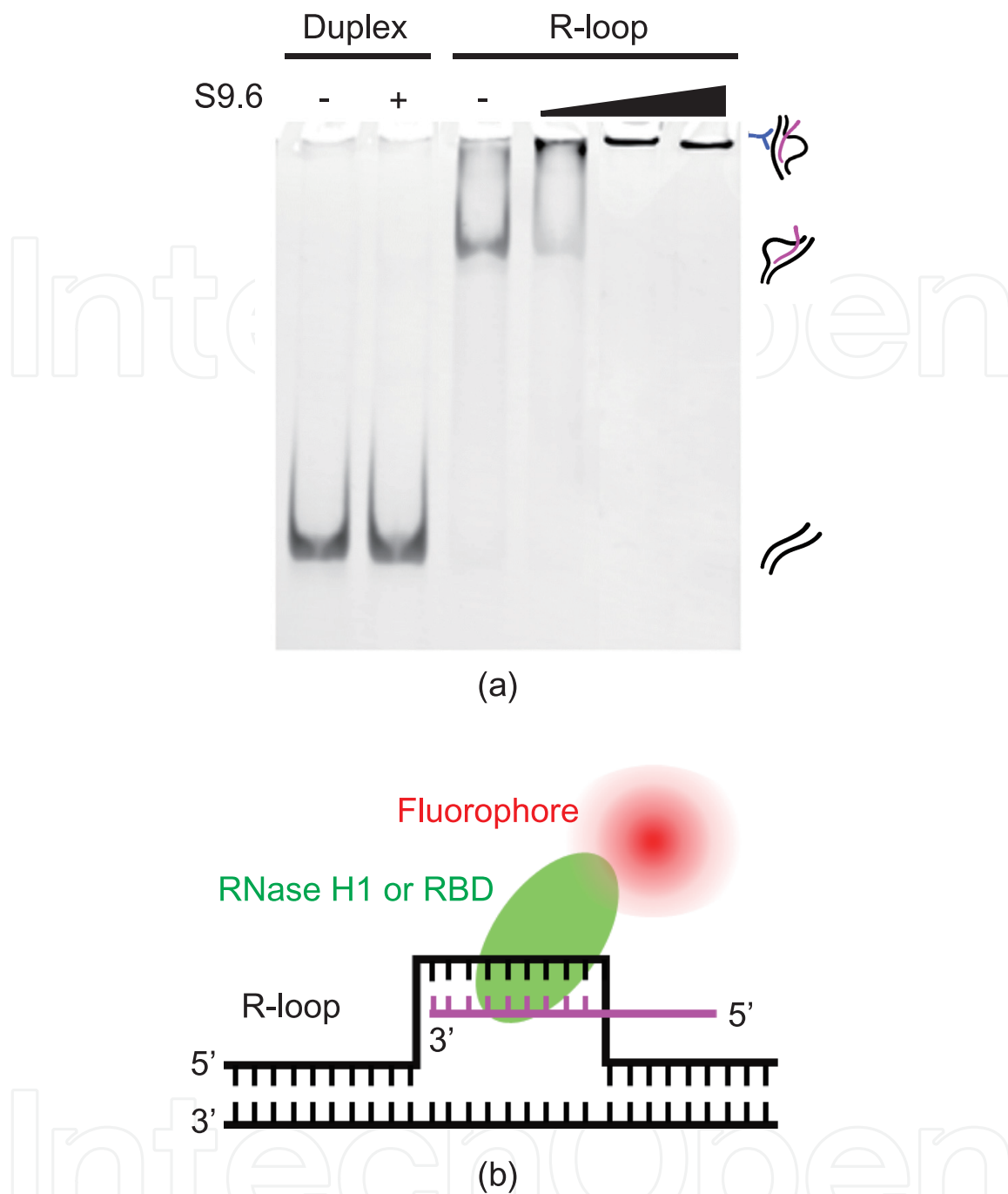
Figure 3.
Flow chart of in vivo *immunofluorescence imaging using S9.6 for R-loop visualization. (a) Flow chart of*
in vivo *immunofluorescence imaging using S9.6 for R-loop visualization. (b) Cellular images of S9.6 labeled with*
fluorescent secondary antibodies. RNase H1 overexpression significantly reduces the S9.6 signal due to elimination
of R-loops.

can also be visualized via R-loop associated proteins with diverse modifications. Prendergast *et al*. subcloned the RNA binding domain (RBD) of RNase H1 fused to DsRed fluorescent protein to monitor intracellular R-loop dynamics [57]. Hodroj *et al*. enhanced green fluorescent protein (eGFP)-fused Ddx19 RNA helicase that specifically binds RNA–DNA hybrids. The fluorescent signal of eGFP-Ddx19 indicates R-loop formation inside cells. In addition, it does not form foci when RBD-mutated Ddx19 and phosphorylation site-mutated Ddx19 are used [58].

3. *In vitro* approaches

In addition to *in vivo* methods, several biochemical assays have been developed to study R-loops. Classically, R-loops are formed from transcription in a supercoiled plasmid by phage RNA polymerases (RNAPs) such as T3 or T7 [59]. Because R-loops have a three-strand structure, they have lower mobility than DNA duplexes in gel electrophoresis, so band shift or smearing occurs between supercoiled and relaxed plasmids during this procedure [53, 60]. Because RNase H digests ssRNA, dsRNA, and RNA–DNA hybrids, RNase H treatment eliminates the mobility shift of plasmids observed with gel electrophoresis [61, 62]. In addition, R-loops can be detected by isotope (e.g. ^{32}P) or fluorescently labeled RNA, which is formed with isotope or fluorescently labeled ribonucleoside triphosphates during transcription. The labeled RNA is used to confirm if the plasmid mobility shift actually results from R-loops [53, 60]. In contrast, S9.6 is also used in electrophoresis mobility shift assay (EMSA) and Western blot with oligomers (**Figure 4a**). EMSA in **Figure 4a** was performed with fluorescently labeled R-loop and homoduplex DNA with synthesized oligomers (**Table 1**) following the previous protocol [55]. The oligomers were mixed for R-loop

Figure 4.
In vitro EMSA (electrophoresis mobility shift assay) for R-loop identification. (a) EMSA image for identifying R-loops in vitro. Fluorescently labeled oligomers were hybridized to form duplex DNA and R-loop structures. The R-loops shifted upward because of their lower mobility compared with same-length duplex DNA due to its molecular weight and the displaced ssDNA (lane 1 vs. lane 3). Because S9.6 specifically binds to R-loops, S9.6 treatment further super-shifts R-loops but not duplexes (lane 2 vs. lanes 4, 5, and 6). The black triangle represents the increasing concentration of S9.6 antibody (10, 30, and 50 nM). (b) Simplified diagram of R-loop visualization using fluorescently labeled catalytically-inactive RNase H1 or RBD. In addition to the S9.6 antibody, catalytically-inactive RNase H1 and RBD with fluorescence dye can also be used to visualize R-loops.

and homoduplex DNA as shown in **Table 2**, and the mixture was heated at 95°C and then slowly cooled down to room temperature. 10 nM R-loop or duplex DNA was mixed to S9.6 (10, 30 and 50 nM) in reaction buffer (10 mM HEPES [pH 7.5], 1 mM DTT, and 5% glycerol). The reactant was incubated in the dark at room temperature for 20 min. The R-loop formation and the binding of S9.6 to R-loop were analyzed with 5% non-denaturing polyacrylamide gel electrophoresis and imaged by Typhoon

Oligomer name	Sequences
DNA 1	5'-GCC GTC GCA TGA CGC TGC CGA ATT CTA CCA CGC GAT TCA TAC CTG TCG TGC CAG CTG CTT TGC CCA CCT GCA GGT TCA CCT CGT CCC TGG C-3'
DNA 2	5'-[Cy3]-GCC AGG GAC GAG GTG AAC CTG CAG GTG GGC AAA GCA GCT GGC ACG ACA GGT ATG AAT CGC GTG GTA GAA TTC GGC AGC GTC ATG CGA CGG C-3'
DNA 3	5'-[Cy3]-GCC AGG GAC GAG GTG AAC CTG CAG GTG GGC GGC TAC TAC TTA GAT GTC ATC CGA GGC TTA TTG GTA GAA TTC GGC AGC GTC ATG C GA CGG C-3'
RNA 1	5'-[Cy5]-GCA GCU GGC ACG ACA GGU AUG AAU C-3'
[Cy3] and [Cy5] indicate the labeling of Cy3 and Cy5 fluorescent dyes, respectively.	

Table 1.
List of oligomers for EMSA.

Substrate name	Mixture recipe (total 20 μl in reaction buffer)
Homoduplex	**DNA 1**: 6 μM, **DNA 2**: 5 μM
R-Loop	**DNA 1**: 6 μM, **DNA 3**: 5 μM, **RNA 1**: 5 μM

Table 2.
Hybridization of oligomers for EMSA.

RGB (GE Healthcare) system. In EMSA using the oligomers, R-loops show band shift from dsDNA resulting from low mobility due to its triple-strand structure. Further band shift is observed following treatment with S9.6, which binds to RNA–DNA hybrids [50, 55]. In Western blotting, RNA–DNA hybrid interactors can be validated using S9.6 and target protein immunoprecipitation [45].

Purified RBD-DsRed specifically binds to RNA-containing structures, enabling its use as a probe of R-loops (**Figure 4b**). DNA fibers can be spread on a surface to distinguish the positions of R-loop regions with the purified RBD-DsRed. Various tags combining the RBD of RNase H1 have been used in microscopic fluorescent imaging, EMSA, and DRIP-seq to identify R-loops [63]. Crossely *et al*. designed and purified different types of RNase H1 that contains RBD and full amino acid sequences [50]. However, the RNase H1 used in their research has a D210N mutation that renders it catalytically inactive. Their construct successfully recognizes R-loops and RNA–DNA hybrids without degradation of RNA in EMSA. The GFP-labeled catalytic mutant RNase H1 thoroughly colocalized with R-loop-containing oligos within the cells.

Atomic force microscopy (AFM) scans a sample on a mica surface using a cantilever to yield a topographic image of the sample [64]. AFM has revealed diverse types of nucleic acids structures and DNA-protein complex formations [65–67]. AFM is also applied for visualizing R-loop formation. Carrasco-Salas *et al*. used AFM to observe three distinct structures derived from R-loops: blobs, spurs, and loops [68]. The specific R-loop structures depend on the sequence of non-template strand that is displaced in the R-loop, which suggests that non-template strand organization is an intrinsic characteristic of R-loops.

4. Single-molecule approaches for R-loop studies

Although R-loop formation, function, and fate have been extensively studied using biochemical assays and cell-based imaging as described above, those

approaches still have limitations related to probing molecular details due to the ensemble average effect. Such hurdles can be overcome with single-molecule techniques that enable researchers to 1) observe individual molecules without an ensemble average effect, 2) mechanically manipulate biomolecules, and 3) directly observe biomolecular interactions [69]. Several single-molecule techniques have been utilized for R-loop studies. Lee *et al*. used protein-induced fluorescence enhancement (PIFE) to observe R-loop formation during T7 RNA polymerase transcription [70]. PIFE is a phenomenon in which a protein sometimes enhances the intensity of fluorescent dyes on other biomolecules [71]. PIFE assays exploit this intensity enhancement to measure the distance and interaction between non-tagged proteins and fluorescent dyes on target molecules, such as DNA. Fluorescent tagging of proteins is inefficient and may disturb protein activity; however, in PIFE assays there is no need to tag proteins [72]. The authors demonstrated that a G-quadruplex on the non-template strand stabilizes the R-loop, which enhances transcription elongation.

In addition to PIFE, single-molecule FRET (smFRET) has been widely used for probing the conformational dynamics of biomolecules (**Figure 5a**) [73, 74]. FRET requires two dyes (donor and acceptor) with spectral overlap for donor emission and acceptor absorption. In FRET, only the donor dye is excited, while the acceptor dye emits fluorescence through energy transfer when both dyes are in close proximity, as the energy transfer efficiency depends on the distance between them. R-loops are also studied using smFRET, during which the target DNA or RNA and RNA polymerases are fluorescently labeled with FRET donors and acceptors (**Figure 5a**, [75]). For smFRET experiments, one DNA oligomer with both FRET donor (Cy3) and acceptor (Cy5) and its complementary oligomer with biotin were hybridized. The hybridized DNA was anchored on the surface of a quartz slide coated with polyethylene glycol (PEG) via biotin-streptavidin interaction. Transcription was initiated by injecting 8 nM T7 RNA polymerases and 2 mM of rNTPs in imaging buffer (40 mM Tris–HCl [pH 8.0], 50 mM KCl, 5 mM NaOH, 20 mM $MgCl_2$, 1 mM DTT, 2 mM spermidine, 3 mM Trolox, 5 mM PCA, and 4 units/ml PCD). Total internal reflection fluorescence (TIRF) microscopy equipped with an electron-multiplying CCD camera was used for fluorescence imaging. Donor (Cy3) and acceptor (Cy5) dyes were excited by 532-nm and 633-nm lasers, respectively. smFRET experiments revealed that R-loop formation precedes and facilitates G-quadruplex formation, which is extremely stable even after R-loop resolution. Using smFRET, we can examine R-loop formation induced by dsDNA denaturation, collision between RNAP and obstacles such as protein roadblocks or DNA lesions, and G-quadruplex formation of displaced ssDNA during R-loop formation [70, 75].

In addition to R-loop formation, sensing R-loops is important for downstream processes, including R-loop resolution. In particular, how R-loop-binding proteins recognize R-loops in long genomic DNA is unclear. R-loop search mechanisms have been investigated with a novel single-molecule fluorescence imaging technique called DNA curtain (**Figure 5b**, [76, 77]). In this assay, DNA molecules are anchored on a lipid bilayer and aligned at nanometric diffusion barriers. Owing to the fluidity of the surface lipid bilayer, DNA molecules are unidirectionally stretched under hydrodynamic flow. DNA curtains can be used to identify sequence-dependent binding of proteins to DNA. Moreover, they allow us to visualize the movement of a protein along a single DNA molecule in real time. To study the search mechanism, an R-loop is inserted into a specific location of lambda phage DNA and fluorescently imaged with Cy5-labeled RNA in the R-loop. Then, the R-loop-binding protein is tagged with a fluorescent nanoparticle called a quantum dot (Qdot), which has a different
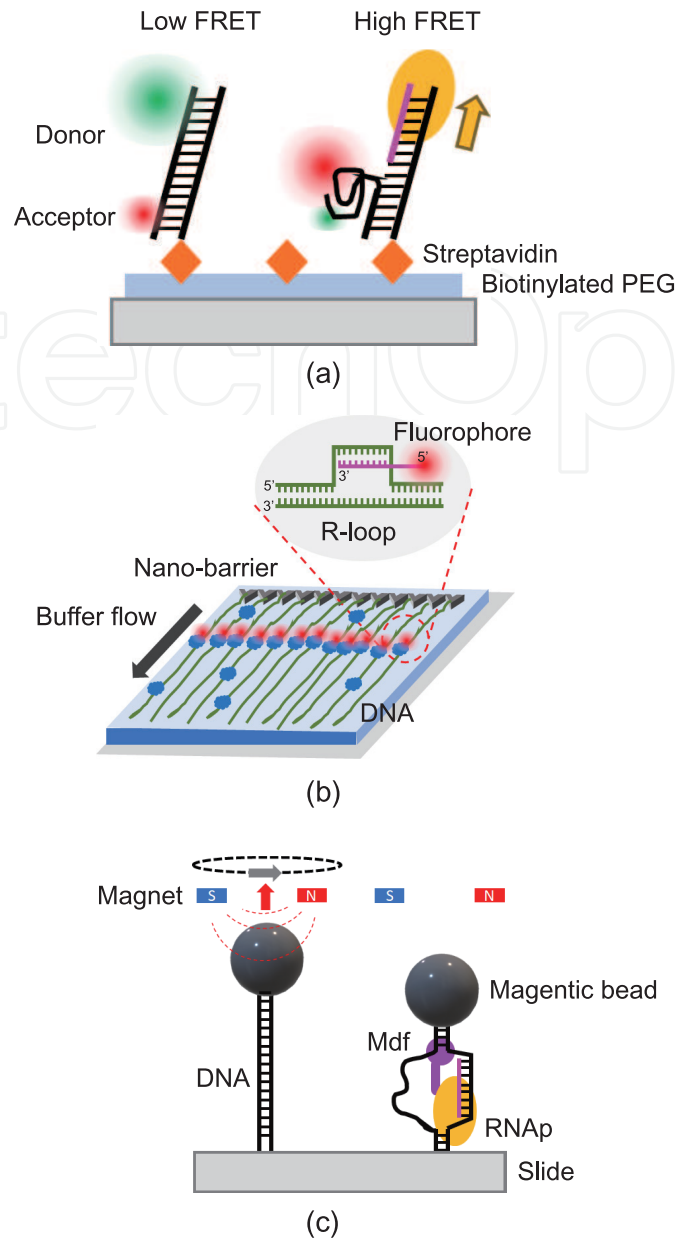
Figure 5.
Single-molecule R-loop visualization techniques. (a) Schematic of single-molecule FRET. Hybridized oligomers are anchored on the biotinylated polyethylene glycol surface via biotin-streptavidin linkage. Donor (green) and acceptor (red) dyes in a duplex DNA display low FRET due to the long distance between the two dyes. However, when an R-loop is formed during the transcription by RNAP (yellow), the dissociated ssDNA emits high FRET. (b) Schematic of single-molecule DNA curtain. For DNA curtain assay, the slide surface with nanometric diffusion barriers was coated with a biotinylated lipid bilayer, which is made of DOPC (1,2-dioleoyl-sn-glycero-phosphocholine), 0.5% biotinylated-DPPE (1,2-dipalmitoyl-sn-glycero-3-phosphoethanolamine-N-(cap biotinyl)), and 8% mPEG 2000-DOPE (1,2-dioleoyl-sn-glycero-3-phosphoethanolamine-N-[methoxy(polyethylene glycol)-2000]). A Cy5-labeled R-loop was inserted into lambda phage DNA, which has biotin at one end. The lambda phage DNA was anchored on the lipid bilayer via biotin-streptavidin linkage in BSA buffer (40 mM Tris–HCl [pH 8.0], 50 mM NaCl, 2 mM MgCl$_2$, and 0.4% BSA). TonEBP with 3x FLAG was labeled with anti-FLAG conjugated quantum dot. Under hydrodynamic flow, DNA curtain was formed in reaction buffer (10 mM HEPES [pH 7.5] and 50 mM NaCl), and R-loops were imaged by Cy5 fluorescence under TIRF microscopy. Then quantum dot-labeled TonEBP was incubated with the lambda DNA, and its binding to the R-loop was imaged. DNA molecules containing an R-loop are unidirectionally stretched on the biotinylated lipid-coated slide (sky blue) and aligned at the chromium nano-barrier (gray) due to the fluidity of lipid bilayer. The interaction between TonEBP (blue) and R-loops (red), in which RNA is labeled with a fluorescent dye, can be visualized in real time. (c) Schematic of magnetic tweezers. The magnetic field exerts and measures both force and torque on the magnetic bead (black). The interaction between Mdf (violet) linked to both duplex DNA and RNAP (yellow) during R-loop formation can be measured based on the length change of DNA under a constant force using magnetic tweezers.

emission wavelength from Cy5. Two-color imaging of both Cy5 and Qdot in the DNA curtain allows the R-loop search mechanism of the R-loop-binding protein. Kang *et al*. reported that tonicity enhancer-binding protein (TonEBP) plays important roles in R-loop sensing and recruitment of downstream proteins [55]. Using the DNA curtain approach, they revealed that TonEBP preferentially binds R-loops through both three-dimensional collision and one-dimensional diffusion. This dual-search mechanism facilitates rapid searches for R-loop throughout the long human genome. Furthermore, the quantitative analysis on one-dimensional diffusion shows that TonEBP diffuses along DNA by sliding rather than hopping. In EMSAs, TonEBP preferentially binds R-loops, D-loops, and bubble DNA structures over duplex DNA. The substances for which TonEBP has a high affinity all contain displaced ssDNA structures. These results indicate that TonEBP preferentially binds displaced ssDNA, thus recognizing R-loops on duplex DNA.

Magnetic tweezers assay can measure both the tension and topological features of a single supercoiled DNA. In this approach, a linear DNA molecule is torsionally constrained by tethering the DNA ends to the slide surface and a magnetic bead that is rotated to induce DNA supercoiling (**Figure 5c**). Portmen *et al*. used magnetic tweezers to elucidate the R-loop formation mechanism by the transcription-coupled repair factor Mfd during transcription based on topologically changing the DNA [78]. For the magnetic tweezers assay, 4.6 kbp long DNA containing a promoter site was ligated with biotinylated handle at one end and digoxigenin handle at the other hand. Digoxigenin end was anchored on an anti-digoxigenin-coated glass coverslip, and biotinylated end was attached to a 1 μm diameter superparamagnetic bead. Transcription reaction was done in reaction buffer (40 mM HEPES [pH 8.0], 100 mM KCl, 8 mM $MgCl_2$, 0.5 mg/ml BSA, and 1 mM DTT) supplemented with 300 pM RNA polymerases, 500 nM Mfd, 50 nM GreB, 1 mM rATP, 100 μM rCTP, 100 μM rUTP, and 100 μM rGTP. They found that R-loop formation was mediated by the Mfd-RNAP complex, which compacted and supercoiled the template DNA during transcription. Mfd simultaneously binds both RNAP and DNA and results in tripartite supercoiled domains. The negative supercoiling in the tripartite domains serves as a substrate for R-loop formation.

With advances in single-molecule imaging technology, we can investigate R-loops and related factors that cannot be observed in traditional ensemble assays. The convergence of single-molecule techniques and R-loop research will pave the way to more thorough investigation of R-loops with higher spatiotemporal resolution.

5. Conclusions

R-loops are involved in various cellular activities but can threaten genomic stability. Detecting these structures is important for understanding their metabolism and underlying mechanism. This chapter described the formation, roles, and regulation of R-loops and related diseases and explored *in vivo* and *in vitro* methods for R-loop detection and visualization, including single-molecule techniques. The most classical methods for R-loop are based on the S9.6 antibody. However, novel techniques that do not require this antibody have been developed. In particular, single-molecule R-loop imaging techniques have accelerated research. We expect that more advanced techniques for R-loops with high sensitivity and resolution will be developed in the future.

Acknowledgements

Conflict of interest

The authors declare no conflict of interest.

Author details

Na Young Cheon[1], Subin Kim[1] and Ja Yil Lee[1,2]*

1 Department of Biological Sciences, Ulsan National Institute of Science and Technology, Ulsan, Republic of Korea

2 Center for Genomic Integrity, Institute for Basic Science, Ulsan, Republic of Korea

*Address all correspondence to: biojayil@unist.ac.kr

IntechOpen

References

[1] Thomas M, White RL, Davis RW. Hybridization of RNA to double-stranded DNA: Formation of R-loops. Proceedings of the National Academy of Sciences of the United States of America. 1976;**73**(7):2294-2298. DOI: 10.1073/pnas.73.7.2294

[2] Roberts RW, Crothers DM. Stability and properties of double and triple helices: Dramatic effects of RNA or DNA backbone composition. Science. 1992;**258**(5087):1463-1466. DOI: 10.1126/science.1279808

[3] Wang AH, Fujii S, van Boom JH, van der Marel GA, van Boeckel SA, Rich A. Molecular structure of r(GCG) d(TATACGC): A DNA--RNA hybrid helix joined to double helical DNA. Nature. 1982;**299**(5884):601-604. DOI: 10.1038/299601a0

[4] Ehara H, Sekine SI. Architecture of the RNA polymerase II elongation complex: New insights into Spt4/5 and Elf1. Transcription. 2018;**9**(5):286-291. DOI: 10.1080/21541264.2018.1454817

[5] Zhang B, Luo D, Li Y, Perculija V, Chen J, Lin J, et al. Mechanistic insights into the R-loop formation and cleavage in CRISPR-Cas12i1. Nature Communications. 2021;**12**(1):3476. DOI: 10.1038/s41467-021-23876-5

[6] Martinez-Rucobo FW, Cramer P. Structural basis of transcription elongation. Biochimica et Biophysica Acta. 2013;**1829**(1):9-19. DOI: 10.1016/j.bbagrm.2012.09.002

[7] Yin YW, Steitz TA. The structural mechanism of translocation and helicase activity in T7 RNA polymerase. Cell. 2004;**116**(3):393-404. DOI: 10.1016/s0092-8674(04)00120-5

[8] Roy D, Zhang Z, Lu Z, Hsieh CL, Lieber MR. Competition between the RNA transcript and the nontemplate DNA strand during R-loop formation in vitro: A nick can serve as a strong R-loop initiation site. Molecular and Cellular Biology. 2010;**30**(1):146-159. DOI: 10.1128/MCB.00897-09

[9] Liu LF, Wang JC. Supercoiling of the DNA template during transcription. Proceedings of the National Academy of Sciences of the United States of America. 1987;**84**(20):7024-7027. DOI: 10.1073/pnas.84.20.7024

[10] Wahba L, Amon JD, Koshland D, Vuica-Ross M. RNase H and multiple RNA biogenesis factors cooperate to prevent RNA:DNA hybrids from generating genome instability. Molecular Cell. 2011;**44**(6):978-988. DOI: 10.1016/j.molcel.2011.10.017

[11] Dominguez-Sanchez MS, Barroso S, Gomez-Gonzalez B, Luna R, Aguilera A. Genome instability and transcription elongation impairment in human cells depleted of THO/TREX. PLoS Genetics. 2011;**7**(12):e1002386. DOI: 10.1371/journal.pgen.1002386

[12] Gomez-Gonzalez B, Garcia-Rubio M, Bermejo R, Gaillard H, Shirahige K, Marin A, et al. Genome-wide function of THO/TREX in active genes prevents R-loop-dependent replication obstacles. The EMBO Journal. 2011;**30**(15):3106-3119. DOI: 10.1038/emboj.2011.206

[13] Huertas P, Aguilera A. Cotranscriptionally formed DNA:RNA hybrids mediate transcription elongation impairment and transcription-associated recombination. Molecular Cell. 2003;**12**(3):711-721. DOI: 10.1016/j.molcel.2003.08.010

[14] Roy D, Yu K, Lieber MR. Mechanism of R-loop formation at immunoglobulin class switch sequences. Molecular and Cellular Biology. 2008;**28**(1):50-60. DOI: 10.1128/MCB.01251-07

[15] Deaton AM, Bird A. CpG islands and the regulation of transcription. Genes & Development. 2011;**25**(10):1010-1022. DOI: 10.1101/gad.2037511

[16] Ginno PA, Lott PL, Christensen HC, Korf I, Chedin F. R-loop formation is a distinctive characteristic of unmethylated human CpG island promoters. Molecular Cell. 2012;**45**(6):814-825. DOI: 10.1016/j. molcel.2012.01.017

[17] Sun Q, Csorba T, Skourti-Stathaki K, Proudfoot NJ, Dean C. R-loop stabilization represses antisense transcription at the Arabidopsis FLC locus. Science. 2013;**340**(6132):619-621. DOI: 10.1126/science.1234848

[18] Boque-Sastre R, Soler M, Oliveira-Mateos C, Portela A, Moutinho C, Sayols S, et al. Head-to-head antisense transcription and R-loop formation promotes transcriptional activation. Proceedings of the National Academy of Sciences of the United States of America. 2015;**112**(18):5785-5790. DOI: 10.1073/pnas.1421197112

[19] Castellano-Pozo M, Santos-Pereira JM, Rondon AG, Barroso S, Andujar E, Perez-Alegre M, et al. R loops are linked to histone H3 S10 phosphorylation and chromatin condensation. Molecular Cell. 2013;**52**(4):583-590. DOI: 10.1016/j. molcel.2013.10.006

[20] Ginno PA, Lim YW, Lott PL, Korf I, Chedin F. GC skew at the 5′ and 3′ ends of human genes links R-loop formation to epigenetic regulation and transcription termination. Genome

Research. 2013;**23**(10):1590-1600. DOI: 10.1101/gr.158436.113

[21] Skourti-Stathaki K, Kamieniarz-Gdula K, Proudfoot NJ. R-loops induce repressive chromatin marks over mammalian gene terminators. Nature. 2014;**516**(7531):436-439. DOI: 10.1038/nature13787

[22] Grzechnik P, Gdula MR, Proudfoot NJ. Pcf11 orchestrates transcription termination pathways in yeast. Genes & Development. 2015;**29**(8):849-861. DOI: 10.1101/gad.251470.114

[23] Skourti-Stathaki K, Proudfoot NJ, Gromak N. Human senataxin resolves RNA/DNA hybrids formed at transcriptional pause sites to promote Xrn2-dependent termination. Molecular Cell. 2011;**42**(6):794-805. DOI: 10.1016/j. molcel.2011.04.026

[24] Balk B, Maicher A, Dees M, Klermund J, Luke-Glaser S, Bender K, et al. Telomeric RNA-DNA hybrids affect telomere-length dynamics and senescence. Nature Structural & Molecular Biology. 2013;**20**(10):1199-1205. DOI: 10.1038/nsmb.2662

[25] Luke B, Panza A, Redon S, Iglesias N, Li Z, Lingner J. The Rat1p 5′ to 3′ exonuclease degrades telomeric repeat-containing RNA and promotes telomere elongation in Saccharomyces cerevisiae. Molecular Cell. 2008;**32**(4):465-477. DOI: 10.1016/j.molcel.2008.10.019

[26] Pfeiffer V, Crittin J, Grolimund L, Lingner J. The THO complex component Thp2 counteracts telomeric R-loops and telomere shortening. The EMBO Journal. 2013;**32**(21):2861-2871. DOI: 10.1038/emboj.2013.217

[27] Basu U, Meng FL, Keim C, Grinstein V, Pefanis E, Eccleston J, et al.

The RNA exosome targets the AID cytidine deaminase to both strands of transcribed duplex DNA substrates. Cell. 2011;**144**(3):353-363. DOI: 10.1016/j.cell.2011.01.001

[28] Li X, Manley JL. Cotranscriptional processes and their influence on genome stability. Genes & Development. 2006;**20**(14):1838-1847. DOI: 10.1101/gad.1438306

[29] Aguilera A, Garcia-Muse T. R loops: From transcription byproducts to threats to genome stability. Molecular Cell. 2012;**46**(2):115-124. DOI: 10.1016/j.molcel.2012.04.009

[30] Richard P, Manley JL. R loops and links to human disease. Journal of Molecular Biology. 2017;**429**(21):3168-3180. DOI: 10.1016/j.jmb.2016.08.031

[31] Reddy K, Tam M, Bowater RP, Barber M, Tomlinson M, Nichol Edamura K, et al. Determinants of R-loop formation at convergent bidirectionally transcribed trinucleotide repeats. Nucleic Acids Research. 2011;**39**(5):1749-1762. DOI: 10.1093/nar/gkq935

[32] Reddy K, Schmidt MH, Geist JM, Thakkar NP, Panigrahi GB, Wang YH, et al. Processing of double-R-loops in (CAG).(CTG) and C9orf72 (GGGGCC).(GGCCCC) repeats causes instability. Nucleic Acids Research. 2014;**42**(16):10473-10487. DOI: 10.1093/nar/gku658

[33] Lim YW, Sanz LA, Xu X, Hartono SR, Chedin F. Genome-wide DNA hypomethylation and RNA:DNA hybrid accumulation in Aicardi-Goutieres syndrome. eLife. 2015;**4**:e08007. DOI: 10.7554/eLife.08007

[34] Powell WT, Coulson RL, Gonzales ML, Crary FK, Wong SS,

Adams S, et al. R-loop formation at Snord116 mediates topotecan inhibition of Ube3a-antisense and allele-specific chromatin decondensation. Proceedings of the National Academy of Sciences of the United States of America. 2013;**110**(34):13938-13943. DOI: 10.1073/pnas.1305426110

[35] Salvi JS, Mekhail K. R-loops highlight the nucleus in ALS. Nucleus. 2015;**6**(1):23-29. DOI: 10.1080/19491034.2015.1004952

[36] Bhatia V, Barroso SI, Garcia-Rubio ML, Tumini E, Herrera-Moyano E, Aguilera A. BRCA2 prevents R-loop accumulation and associates with TREX-2 mRNA export factor PCID2. Nature. 2014;**511**(7509):362-365. DOI: 10.1038/nature13374

[37] Hatchi E, Skourti-Stathaki K, Ventz S, Pinello L, Yen A, Kamieniarz-Gdula K, et al. BRCA1 recruitment to transcriptional pause sites is required for R-loop-driven DNA damage repair. Molecular Cell. 2015;**57**(4):636-647. DOI: 10.1016/j.molcel.2015.01.011

[38] Costantino L, Koshland D. Genome-wide map of R-loop-induced damage reveals how a subset of R-loops contributes to genomic instability. Molecular Cell. 2018;**71**(4):487-97 e3. DOI: 10.1016/j.molcel.2018.06.037

[39] Cerritelli SM, Crouch RJ. Ribonuclease H: The enzymes in eukaryotes. The FEBS Journal. 2009;**276**(6):1494-1505. DOI: 10.1111/j.1742-4658.2009.06908.x

[40] Hamperl S, Cimprich KA. The contribution of co-transcriptional RNA:DNA hybrid structures to DNA damage and genome instability. DNA Repair (Amst). 2014;**19**:84-94. DOI: 10.1016/j.dnarep.2014.03.023

[41] Drolet M, Bi X, Liu LF. Hypernegative supercoiling of the DNA template during transcription elongation in vitro. The Journal of Biological Chemistry. 1994;**269**(3):2068-2074

[42] Okamoto Y, Abe M, Itaya A, Tomida J, Ishiai M, Takaori-Kondo A, et al. FANCD2 protects genome stability by recruiting RNA processing enzymes to resolve R-loops during mild replication stress. The FEBS Journal. 2019;**286**(1):139-150. DOI: 10.1111/febs.14700

[43] Boguslawski SJ, Smith DE, Michalak MA, Mickelson KE, Yehle CO, Patterson WL, et al. Characterization of monoclonal antibody to DNA.RNA and its application to immunodetection of hybrids. Journal of Immunological Methods. 1986;**89**(1):123-130. DOI: 10.1016/0022-1759(86)90040-2

[44] Kotsantis P, Silva LM, Irmscher S, Jones RM, Folkes L, Gromak N, et al. Increased global transcription activity as a mechanism of replication stress in cancer. Nature Communications. 2016;**7**:13087. DOI: 10.1038/ncomms13087

[45] Cristini A, Groh M, Kristiansen MS, Gromak N. RNA/DNA hybrid Interactome identifies DXH9 as a molecular player in transcriptional termination and R-loop-associated DNA damage. Cell Reports. 2018;**23**(6):1891-1905. DOI: 10.1016/j.celrep.2018.04.025

[46] Arab K, Karaulanov E, Musheev M, Trnka P, Schafer A, Grummt I, et al. GADD45A binds R-loops and recruits TET1 to CpG island promoters. Nature Genetics. 2019;**51**(2):217-223. DOI: 10.1038/s41588-018-0306-6

[47] Sanz LA, Castillo-Guzman D, Chedin F. Mapping R-loops and RNA:DNA hybrids with S9.6-based immunoprecipitation methods. Journal of Visualized Experiments. 2021;**174**. DOI: 10.3791/62455

[48] Sanz LA, Chedin F. High-resolution, strand-specific R-loop mapping via S9.6-based DNA-RNA immunoprecipitation and high-throughput sequencing. Nature Protocols. 2019;**14**(6):1734-1755. DOI: 10.1038/s41596-019-0159-1

[49] Wahba L, Costantino L, Tan FJ, Zimmer A, Koshland D. S1-DRIP-seq identifies high expression and polyA tracts as major contributors to R-loop formation. Genes & Development. 2016;**30**(11):1327-1338. DOI: 10.1101/gad.280834.116

[50] Crossley MP, Bocek MJ, Hamperl S, Swigut T, Cimprich KA. qDRIP: A method to quantitatively assess RNA-DNA hybrid formation genome-wide. Nucleic Acids Research. 2020;**48**(14):e84. DOI: 10.1093/nar/gkaa500

[51] Malig M, Hartono SR, Giafaglione JM, Sanz LA, Chedin F. Ultra-deep coverage single-molecule R-loop Footprinting reveals principles of R-loop formation. Journal of Molecular Biology. 2020;**432**(7):2271-2288. DOI: 10.1016/j.jmb.2020.02.014

[52] Malig M, Chedin F. Characterization of R-loop structures using single-molecule R-loop Footprinting and sequencing. Methods in Molecular Biology. 2020;**2161**:209-228. DOI: 10.1007/978-1-0716-0680-3_15

[53] Yu K, Chedin F, Hsieh CL, Wilson TE, Lieber MR. R-loops at immunoglobulin class switch regions in the chromosomes of stimulated B cells. Nature Immunology. 2003;**4**(5):442-451. DOI: 10.1038/ni919

[54] Silva S, Camino LP, Aguilera A. Human mitochondrial degradosome

prevents harmful mitochondrial R loops and mitochondrial genome instability. Proceedings of the National Academy of Sciences of the United States of America. 2018;**115**(43):11024-11029. DOI: 10.1073/pnas.1807258115

[55] Kang HJ, Cheon NY, Park H, Jeong GW, Ye BJ, Yoo EJ, et al. TonEBP recognizes R-loops and initiates m6A RNA methylation for R-loop resolution. Nucleic Acids Research. 2021;**49**(1):269-284. DOI: 10.1093/nar/gkaa1162

[56] Sollier J, Stork CT, Garcia-Rubio ML, Paulsen RD, Aguilera A, Cimprich KA. Transcription-coupled nucleotide excision repair factors promote R-loop-induced genome instability. Molecular Cell. 2014;**56**(6):777-785. DOI: 10.1016/j.molcel.2014.10.020

[57] Prendergast L, McClurg UL, Hristova R, Berlinguer-Palmini R, Greener S, Veitch K, et al. Resolution of R-loops by INO80 promotes DNA replication and maintains cancer cell proliferation and viability. Nature Communications. 2020;**11**(1):4534. DOI: 10.1038/s41467-020-18306-x

[58] Hodroj D, Recolin B, Serhal K, Martinez S, Tsanov N, Abou Merhi R, et al. An ATR-dependent function for the Ddx19 RNA helicase in nuclear R-loop metabolism. The EMBO Journal. 2017;**36**(9):1182-1198. DOI: 10.15252/embj.201695131

[59] Zaychikov E, Denissova L, Heumann H. Translocation of the Escherichia coli transcription complex observed in the registers 11 to 20: "jumping" of RNA polymerase and asymmetric expansion and contraction of the "transcription bubble". Proceedings of the National Academy of Sciences of the United States of America. 1995;**92**(5):1739-1743. DOI: 10.1073/pnas.92.5.1739

[60] Daniels GA, Lieber MR. RNA:DNA complex formation upon transcription of immunoglobulin switch regions: Implications for the mechanism and regulation of class switch recombination. Nucleic Acids Research. 1995;**23**(24):5006-5011. DOI: 10.1093/nar/23.24.5006

[61] Allison DF, Wang GG. R-loops: Formation, function, and relevance to cell stress. Cell Stress. 2019;**3**(2):38-46. DOI: 10.15698/cst2019.02.175

[62] Chon H, Vassilev A, DePamphilis ML, Zhao Y, Zhang J, Burgers PM, et al. Contributions of the two accessory subunits, RNASEH2B and RNASEH2C, to the activity and properties of the human RNase H2 complex. Nucleic Acids Research. 2009;**37**(1):96-110. DOI: 10.1093/nar/gkn913

[63] Wang K, Wang H, Li C, Yin Z, Xiao R, Li Q, et al. Genomic profiling of native R loops with a DNA-RNA hybrid recognition sensor. Science Advances. 2021;**7**(8):eabe3516. DOI: 10.1126/sciadv.abe3516

[64] Ohnesorge F, Binnig G. True atomic resolution by atomic force microscopy through repulsive and attractive forces. Science. 1993;**260**(5113):1451-1456. DOI: 10.1126/science.260.5113.1451

[65] Lyubchenko YL, Gall AA, Shlyakhtenko LS. Visualization of DNA and protein-DNA complexes with atomic force microscopy. Methods in Molecular Biology. 2014;**1117**:367-384. DOI: 10.1007/978-1-62703-776-1_17

[66] Lyubchenko YL, Shlyakhtenko LS. Imaging of DNA and protein-DNA complexes with atomic force microscopy. Critical Reviews in Eukaryotic Gene Expression. 2016;**26**(1):63-96. DOI: 10.1615/CritRevEukaryotGeneExpr.v26.i1.70

[67] Bustamante C, Vesenka J, Tang CL, Rees W, Guthold M, Keller R. Circular DNA molecules imaged in air by scanning force microscopy. Biochemistry. 1992;**31**(1):22-26. DOI: 10.1021/bi00116a005

[68] Carrasco-Salas Y, Malapert A, Sulthana S, Molcrette B, Chazot-Franguiadakis L, Bernard P, et al. The extruded non-template strand determines the architecture of R-loops. Nucleic Acids Research. 2019;**47**(13):6783-6795. DOI: 10.1093/nar/gkz341

[69] Kim SO, Jackman JA, Mochizuki M, Yoon BK, Hayashi T, Cho NJ. Correlating single-molecule and ensemble-average measurements of peptide adsorption onto different inorganic materials. Physical Chemistry Chemical Physics. 2016;**18**(21):14454-14459. DOI: 10.1039/c6cp01168c

[70] Lee CY, McNerney C, Ma K, Zhao W, Wang A, Myong S. R-loop induced G-quadruplex in non-template promotes transcription by successive R-loop formation. Nature Communications. 2020;**11**(1):3392. DOI: 10.1038/s41467-020-17176-7

[71] Hwang H, Kim H, Myong S. Protein induced fluorescence enhancement as a single molecule assay with short distance sensitivity. Proceedings of the National Academy of Sciences of the United States of America. 2011;**108**(18):7414-7418. DOI: 10.1073/pnas.1017672108

[72] Hwang H, Myong S. Protein induced fluorescence enhancement (PIFE) for probing protein-nucleic acid interactions. Chemical Society Reviews. 2014;**43**(4):1221-1229. DOI: 10.1039/c3cs60201j

[73] Ha T. Single-molecule fluorescence resonance energy transfer. Methods. 2001;**25**(1):78-86. DOI: 10.1006/meth.2001.1217

[74] Roy R, Hohng S, Ha T. A practical guide to single-molecule FRET. Nature Methods. 2008;**5**(6):507-516. DOI: 10.1038/nmeth.1208

[75] Lim G, Hohng S. Single-molecule fluorescence studies on cotranscriptional G-quadruplex formation coupled with R-loop formation. Nucleic Acids Research. 2020;**48**(16):9195-9203. DOI: 10.1093/nar/gkaa695

[76] Collins BE, Ye LF, Duzdevich D, Greene EC. DNA curtains: Novel tools for imaging protein-nucleic acid interactions at the single-molecule level. Methods in Cell Biology. 2014;**123**:217-234. DOI: 10.1016/B978-0-12-420138-5.00012-4

[77] Greene EC, Wind S, Fazio T, Gorman J, Visnapuu ML. DNA curtains for high-throughput single-molecule optical imaging. Methods in Enzymology. 2010;**472**:293-315. DOI: 10.1016/S0076-6879(10)72006-1

[78] Portman JR, Brouwer GM, Bollins J, Savery NJ, Strick TR. Cotranscriptional R-loop formation by Mfd involves topological partitioning of DNA. Proceedings of the National Academy of Sciences of the United States of America. 2021;**118**(15):e2019630118. DOI: 10.1073/pnas.2019630118